

# **Investigation of the mechanism of transdermal penetration enhancer- a comparison of multiphoton microscopy and electron microscopy**

Sung-Jan Lin<sup>1,2</sup>, Jin-Ning Lee<sup>3</sup>, Chiao-Ying Lin<sup>4</sup>, Chih-Chieh Chan<sup>1,2</sup>, Ming-Gu Lin<sup>3</sup>, Chun-Chin Wang<sup>3</sup>, Hsin-Yuan Tan<sup>1,5</sup>, Tsung-Hua Tsai<sup>6</sup>, Shiou-Hwa Jee<sup>2</sup>, Chen-Yuan Dong<sup>3</sup>

<sup>1</sup> Institute of Biomedical Engineering, National Taiwan University, Taipei, Taiwan

<sup>2</sup> Department of Dermatology, National Taiwan University Hospital and College of Medicine, Taipei, Taiwan.

<sup>3</sup> Department of Physics, National Taiwan University, Taipei, Taiwan.

<sup>4</sup> Department of Electrical Engineering, National Taiwan University, Taipei, Taiwan

<sup>5</sup> Department of Ophthalmology, Chang Gung Memorial Hospital, Linko, Taiwan

<sup>6</sup> Department of Dermatology, Far Eastern Memorial Hospital, Taipei, Taiwan

## **Abstract**

The aim of this study is to characterize the ability of multiphoton microscopy in monitoring the transdermal penetration enhancing effect of a depilatory agent and the associated structural alterations of stratum corneum. The result is compared with the electron microscopic findings. Our results show that the penetration of both hydrophilic and hydrophobic agents can be enhanced. The morphology of corneocytes becomes a homogenized pattern with focal detachment of surface corneocytes. In combination with Nile red staining, multiphoton imaging also shows that the regular motar-like distribution of lipid matrix was disrupted into a homogenized pattern of lipid distribution. These results are well correlated with the findings of ultrastructural analysis by electron micrographs showing disintegration of the protein envelope of coenocytes, disruption of intracellular keratin and loss of the regular lamellar packing of intercellular lipids. We conclude that, in addition to quantifying the permeation profiles of model drugs, multiphoton microscopy is able to detect the penetration enhancer-induced structural alterations of stratum corneum.

Keywords: transdermal drug delivery, depilatory agent, stratum corneum, ultrastructure, multiphoton microscopy, electron microscopy

Address correspondence to: S.J.L. at [drsjlin@ntu.edu.tw](mailto:drsjlin@ntu.edu.tw) and

C.Y.D. at [cydong@phys.ntu.edu.tw](mailto:cydong@phys.ntu.edu.tw)

## Introduction

Barrier function is one of the most important functions of skin. The outermost layer of skin, stratum corneum, contributes to most of this protective function due to its unique chemical composition and delicate structures.<sup>1</sup> In addition to avoiding water loss from the body surface, it also protects our body from the potential insults from environmental toxic or irritant agents.

Structurally, stratum corneum barrier can be divided into two compartments: protein rich corneocytes embedded in continuous intercellular lipids.<sup>2</sup> A brick and mortar model has long been proposed to depict this specialized structure- corneocytes as the brick and mortar as the intercellular lipids. Corneocytes have peripheral disulfide bond-rich cornified cell envelope (CE). Keratin filaments, rich in intermolecular disulfide bond cross-links, are the major intracellular structural proteins of the corneocytes and are linked to the inner surface of the CE. On the outer surface of corneocytes exists a thin layer of lipid envelope (LE). LE is covalently anchored to the CE and also interacts with intercellular lipid lamellae. The regular compact packing of the intercellular lipid lamellae is key to the barrier function, rendering intercellular space of stratum corneum impermeable.

Therapeutically, drug delivery via transcutaneous route is of great interest due to its easy accessibility, increased patient compliance, and avoidance of possible drug degradation via parental route delivery.<sup>3,4</sup> However, the barrier function of skin also hinders transcutaneous penetration of molecules. To increase the permeation of drugs across skin, various approaches aimed at reversibly reducing the resistance of stratum corneum to drug penetration have been investigated.<sup>5</sup> Among the penetration enhancing agents and methods, chemical penetration enhancers can theoretically increase drug permeation by disrupting either one of or the combination of the intercellular lipid lamellae, intracellular keratin, and intercellular linking proteins of stratum corneum.<sup>6</sup>

Depilatory creams, composed of potassium thioglycolate or calcium thioglycolate in base, have been widely used for removal of unwanted hair for decades. The thioglycolate composition of a depilatory cream can disrupt the disulfide bonds of hair keratin and the weakened hair keratin can be removed by gentle rubbing. Interestingly, depilatory creams have been identified as a unique enhancer for transcutaneous drug delivery.<sup>7-9</sup> By the pretreatment of a depilatory agent, the transdermal penetration of theophylline and even insulin can be greatly enhanced in rats.<sup>7-9</sup> The penetration enhancing effect of a depilatory agent can persist for one day.<sup>9</sup> This suggests that the structural alterations induced by the treatment of a depilatory agent can not fully recover within a window of one day. This is of great clinical significance in terms of the convenience, because the drug of interest can be efficiently delivered without the repeated applications of the depilatory within this window. However, like a double-edged sword, this window may also predispose depilatory

cream users to a higher risk of transcutaneous absorption of toxic agents from the environment. Up to date, the mechanism of depilatory as a penetration enhancer has not been characterized.

Multiphoton microscopy utilizing femtosecond laser for non-linear excitation of fluorescent molecules has been applied to the field of dermatological imaging.<sup>10-12</sup> Recently, it is also applied to the dynamical analysis of percutaneous drug delivery.<sup>13,14</sup> Conventionally, the structural alterations of stratum corneum associated with chemical penetration enhancers are investigated by electron microscopy and the quantification of drug penetration is determined by diffusion chamber.<sup>15</sup>

The aim of this study is to characterize the ability of multiphoton microscopy in monitoring the transdermal penetration enhancing effect of a depilatory agent and the associated structural alterations of stratum corneum. We employed multiphoton imaging to examine its effect on the transepidermal delivery of model fluorescent drugs. The associated changes of corneocytes and intercellular lipid lamellae were also examined by histology, Nile red staining and electron microscopy employing post-fixation with ruthenium tetroxide.

## **Materials and methods**

Foreskin specimens obtained from young adults undergoing routine circumcision were used in this study. The experimental protocol was approved by an Institutional Review Board and informed consent was obtained from each individual. The skin was stored at -80°C and utilized within 2 weeks. Before the each experiment, skin specimens were thawed at room temperature and cut into pieces of about 2.25 cm<sup>2</sup>. In the depilatory treated group, a commercially available depilatory cream (Neet, Reckitt & Colman) was gently applied to the epidermal side of the skin specimen. After 10 mins, the depilatory was removed by gentle rinse in phosphate buffered saline (PBS). In the non-treated skin, skin specimens were treated the same except the depilatory was replaced by PBS.

Two fluorescent molecules (Molecular Probes, Eugene, OR, USA), hydrophobic rhodamine B hexyl ester perchlorate (RBHE) and hydrophilic sulforhodamine B (SRB) were chosen as model drugs in this study. Donor solutions of SRB and RBHE were prepared at 0.005 mg/ml in PBS for determination of the diffusion profiles of each drug. To investigate the penetration profile of fluorescent probes, each experiment is divided into four groups: depilatory treated skin + RBHE, non-treated skin + RBHE, depilatory treated skin + SRB, non-treated skin + SRB. Skin specimens were mounted in a home-made diffusion cell as we previously described.<sup>16</sup> Skin specimens were left in contact with donor solutions in the diffusion cells for 12 hr. Then the skin specimens were removed and washed with PBS to remove the excess donor solutions on the surface of skin specimens before being viewed under a multiphoton microscope.

The setup of the microscope is modified from the multiphoton microscope we described previously.<sup>17</sup> Briefly, the 780-nm output from a titanium-sapphire laser (Tsunami, Spectra Physics, Mountain View, California) pumped by a diode-pumped solid-state laser (Millennia X, Spectra Physics) was used for excitation. The laser was scanned by an *x-y* mirror scanning system (Model 6220, Cambridge Technology, Cambridge, Massachusetts) and guided toward the modified inverted microscope. The laser was beam expanded and reflected into an oil immersion objective (S Fluor, NA 1.3, Nikon) by a primary dichroic mirror (700DCSPXRUV-3p, Chroma Technology, Rockingham, Vermont). Sample luminescence was collected in the epi-illuminated geometry. After passing through the primary dichroic mirror, the second harmonic generation (SHG) and fluorescence signals are separated into four simultaneous detection channels by secondary dichroic mirrors (435DCXR, 495DCXR, 555DCLP, Chroma Technology) and additional bandpass filters (HQ390/20, HQ460/50, HQ525/50, HQ590/80, Chroma Technology). The detection bandwidths for the second harmonic generation (SHG), blue, green, and red fluorescence are  $390\pm 10$ ,  $460\pm 25$ ,  $525\pm 25$ , and  $590\pm 40$  nm, respectively. Autofluorescence signals of 500-550 nm were utilized for observation of morphological alterations after the treatment of a depilatory cream. For investigation of penetration profile of fluorescent model drugs, fluorescence signals of 550-630 nm from SRB and RBHE were collected for analysis. For image processing, we used the software of ImageJ (National Institute of Health, Bethesda, Maryland).

The depilatory treated and non-treated skin specimens were processed for histological examination. Thin frozen sections of the specimens (5 $\mu$ m thick) were obtained and air dried in room temperature before the Hematoxylin and Eosin (H&E) staining. For the observation of the lipid distribution in stratum corneum, Nile red staining was performed as previously described.<sup>18</sup> Briefly, the stock solution of Nile red (Molecular Probes, Inc.) (500  $\mu$ g/ml in acetone) was prepared, stored at -20°C and protected from light exposure. A fresh Nile red staining solution was prepared by adding 15  $\mu$ l stock solution to 1 ml of 75% glycerol, followed by vortexing. For staining, a drop of staining solution was added to frozen sections (5  $\mu$ m thick) of each specimen. After 10 min at room temperature in darkness, the sections were rinsed in distilled water, followed by the treatment of a drop of 4% KOH solution for 2 min. The excess KOH was then wiped off, and the sections were mounted in glycerol and examined by the multiphoton microscope.

To visualize the alignment of intercellular lipid of stratum corneum, the skin specimen was processed for electron microscopic examination as previously described.<sup>19</sup> Each skin specimen was cut into 1-mm pieces and first fixed in the solution of 2.5% glutaraldehyde in cacodylate buffer for 2 hours. The specimens were then post-fixed in 0.2% ruthenium tetroxide in cacodylate buffer for 1 hour. The specimens were then serially dehydrated in a series of ethanol solutions before being embedded in Spurr's resin. Ultrathin sectioning was performed. The sections were floated onto

carbon-stabilized Formvar-coated grids and stained with uranyl acetate and lead citrate before the examination in a Hitachi model H-7501ss electron microscope.

### Results and discussion

**Figure 1** and **Figure 2** show the penetration profile of the hydrophilic model drug SRB and hydrophobic RBHE. The normalized average photon counts per pixel are plotted vs the corresponding skin depth from the surface. The penetration of hydrophilic model drug SRB is increased in the skin specimen pretreated with a depilatory agent (**Figure 1**). From the surface down to the depth of 30 $\mu\text{m}$ , the average fluorescent density of SRB is higher in the depilatory pretreated skin specimen as compared with the control specimen. Similar to SRB, the penetration of hydrophobic RBHE is also increased in the skin specimen pretreated with a depilatory agent (**Figure 2**).

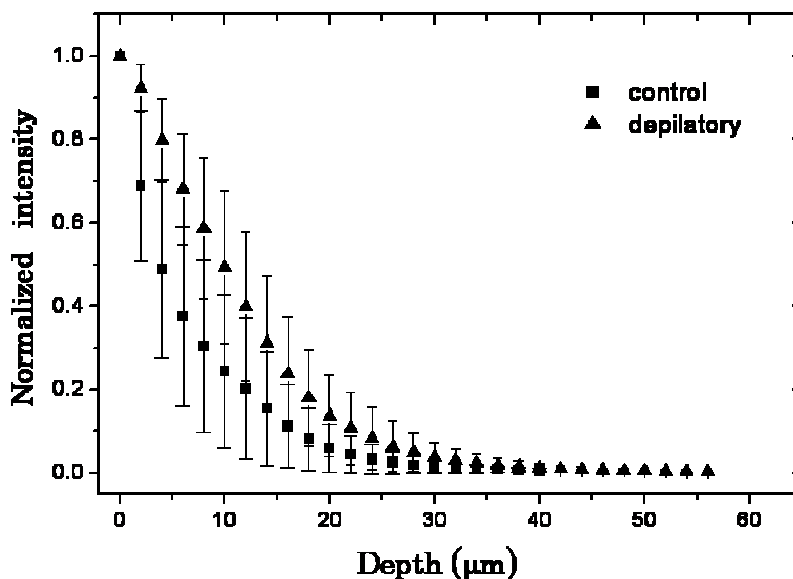


**Figure 1. Penetration profile of SRB.**

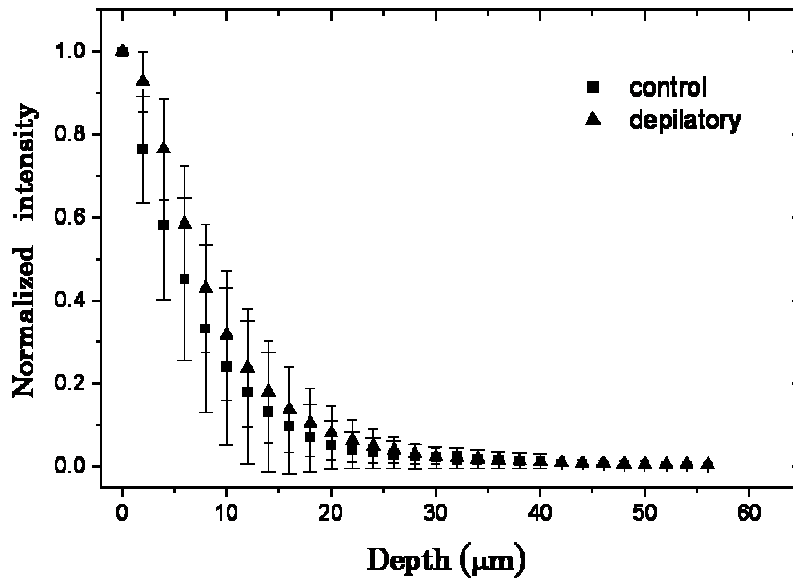


**Figure 2. Penetration profile of RBHE.**

**Figure 3** shows the multiphoton images of stratum corneum from depilatory cream treated and non-depilatory cream treated skin specimens. The autofluorescence from the corneocytes allows direct imaging without any fixation or staining procedures. In the control group (**Figure 3a**), corneocytes are tightly packed as hexagonal cells with distinctive intercellular borders. When the skin is treated by a depilatory cream, stratum corneum becomes a homogenized morphology and intercellular borders can not be clearly delineated. The results show that the structures of corneocytes are disrupted altered by the treatment of a depilatory agent.

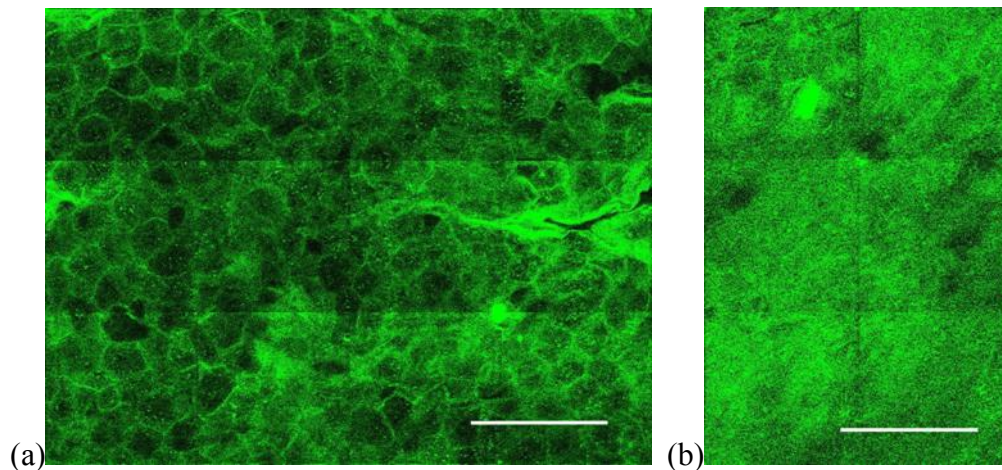


**Figure 3. Multiphoton imaging of stratum corneum.** (a) Control skin specimen (b) Depilatory

treated skin specimen. (bar: 100 $\mu$ m)

**Figure 4** shows the lipid structures by Nile red staining. In the control group (**Figure 4a**), intercellular lipid can be seen as yellow fluorescent matrix surrounding the halo flat corneocytes. After the treatment of a depilatory agent, the intercellular lipid organization was disrupted into a homogenized pattern in the stratum corneum (**Figure 4b**).

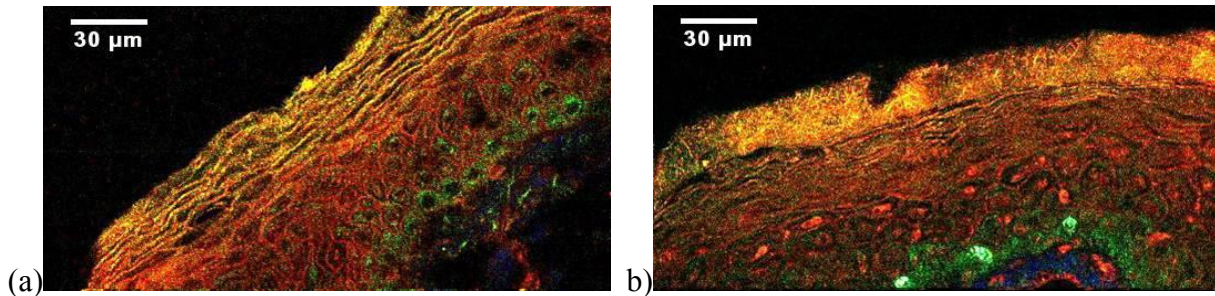


**Figure 4. Multiphoton images of Nile red staining.** (a) Control skin specimen (b) Depilatory treated skin specimen. (bar: 30 $\mu$ m)

**Figure 5** shows the electron micrographs of intracellular structures and intercellular lipid structures of stratum corneum. In the control group (**Figure 5a**), regular packing of intercellular lamellae can be seen and the intact intracellular keratin matrix is observed. In the intercellular space, lipids are regularly packed as multilayered structures. The intercellular lipids are anchored on the electron-dense cornified cell envelope. In the depilatory cream treated skin (**Figure 5b**), the intracellular keratin matrix is disrupted and keratin is lost in the intracellular compartment of some corneocytes. It is also notable that the electron dense cornified cell envelope often become fractured and separated from the intracellular keratin network. The regular packing of multilamellar structure of intercellular lipid is lost.

These results of multiphoton images are well correlated with the findings of ultrastructural analysis by electron micrographs showing disintegration of the protein envelope of corneocytes, disruption of intracellular keratin and loss of the regular lamellar packing of intercellular lipids. The results also demonstrate the ability of a depilatory agent to enhance the transepidermal penetration of both the hydrophilic and hydrophobic models drugs. The pretreatment of a depilatory agent disrupts the structural integrity of both corneocytes and intercellular lipid lamellae of the stratum corneum.

The compact intracellular keratin matrix of corneocytes is disrupted. The disruption of regular packing of intercellular lipid structures can also contribute to the enhanced drug permeation by reducing the resistance to the drug penetration through the intercellular route of stratum corneum.

We conclude that, in addition to quantifying the permeation profiles of model drugs, multiphoton microscopy is able to detect the penetration enhancer-induced structural alterations of stratum corneum.

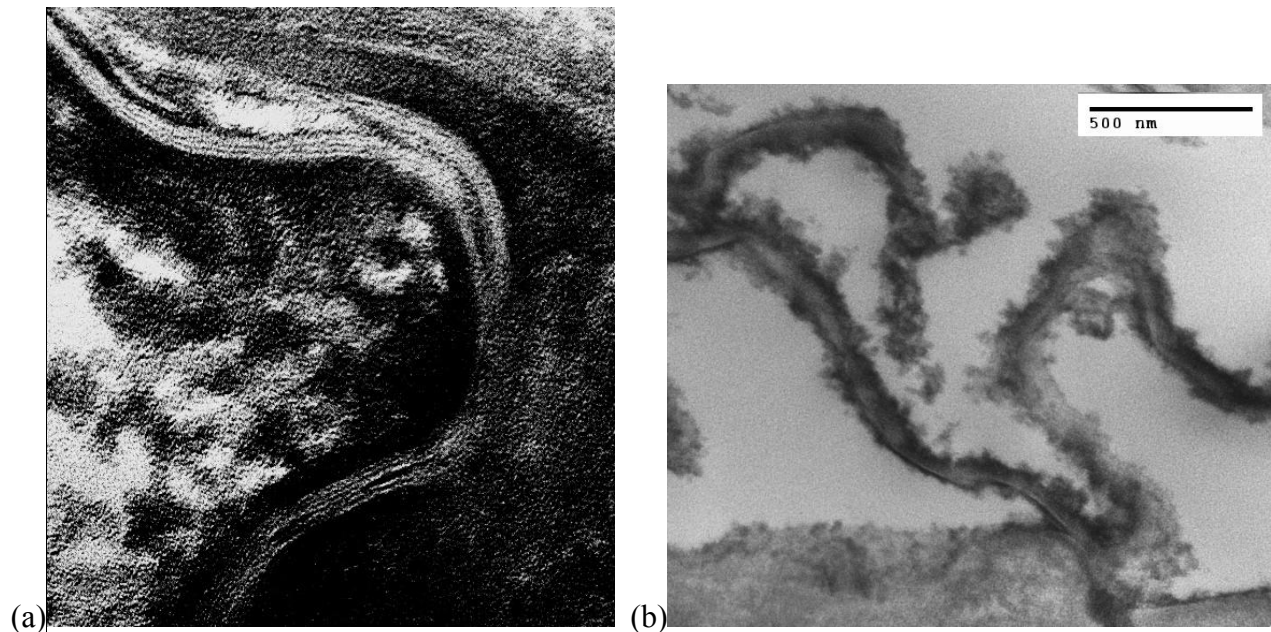


**Figure 5. Electron micrographs of stratum corneum.** (a) Control skin specimen (b) Depilatory treated skin specimen.

### Acknowledgement

Support for this work is provided by the National Research Program for Genomic Medicine of the National Science Council, Taiwan ((NSC-96-3112-B-002-025, NSC-95-3112-B-002-019 and NSC-94-3112-B-002-015Y). The experiments and data analysis involving multiphoton microscopy were performed in the Optical and Scanning Probe Microscopy Core Facility, National Research Program for Genomic Medicine, Taiwan.

### Reference

1. Madison KC (2003) Barrier function of the skin: "la raison d'etre" of the epidermis. *The Journal*



*of investigative dermatology* 121:231-241

2. Elias PM (1983) Epidermal lipids, barrier function, and desquamation. *The Journal of investigative dermatology* 80 Suppl:44s-49s.
3. Balfour JA, Heel RC (1990) Transdermal estradiol. A review of its pharmacodynamic and pharmacokinetic properties, and therapeutic efficacy in the treatment of menopausal complaints. *Drugs* 40:561-582
4. Cevc G (2003) Transdermal drug delivery of insulin with ultradeformable carriers. *Clinical pharmacokinetics* 42:461-474.
5. Williams AC, Barry BW (2004) Penetration enhancers. *Adv Drug Deliv Rev* 56:603-618.
6. Barry BW (2004) Breaching the skin's barrier to drugs. *Nature biotechnology* 22:165-167.
7. Kanikkannan N, Singh J, Ramarao P (1999) Transdermal iontophoretic delivery of bovine insulin and monomeric human insulin analogue. *J Control Release* 59:99-105.
8. Kushida K, Masaki K, Matsumura M, Ohshima T, Yoshikawa H, Takada K, et al. (1984) Application of calcium thioglycolate to improve transdermal delivery of theophylline in rats. *Chemical & pharmaceutical bulletin* 32:268-274.
9. Zakzewski CA, Wasilewski J, Cawley P, Ford W (1998) Transdermal delivery of regular insulin to chronic diabetic rats: effect of skin preparation and electrical enhancement. *J Control Release* 50:267-272.
10. Lin SJ, Jee SH, Dong CY (2007) Multiphoton microscopy: a new paradigm in dermatological imaging. *Eur J Dermatol* 17:361-366.
11. Lin SJ, Jee SH, Kuo CJ, Wu RJ, Lin WC, Chen JS, et al. (2006b) Discrimination of basal cell carcinoma from normal dermal stroma by quantitative multiphoton imaging. *Optics letters* 31:2756-2758.
12. Lin SJ, Wu R, Jr., Tan HY, Lo W, Lin WC, Young TH, et al. (2005) Evaluating cutaneous photoaging by use of multiphoton fluorescence and second-harmonic generation microscopy. *Optics letters* 30:2275-2277.
13. Yu B, Dong CY, So PT, Blankschtein D, Langer R (2001) In vitro visualization and quantification of oleic acid induced changes in transdermal transport using two-photon fluorescence microscopy. *The Journal of investigative dermatology* 117:16-25.
14. Yu B, Kim KH, So PT, Blankschtein D, Langer R (2003) Visualization of oleic acid-induced transdermal diffusion pathways using two-photon fluorescence microscopy. *The Journal of investigative dermatology* 120:448-455.
15. Swartzendruber DC, Burnett IH, Wertz PW, Madison KC, Squier CA (1995) Osmium tetroxide and ruthenium tetroxide are complementary reagents for the preparation of epidermal samples for transmission electron microscopy. *The Journal of investigative dermatology* 104:417-420.

16. Sun Y, Lo W, Lin SJ, Jee SH, Dong CY (2004) Multiphoton polarization and generalized polarization microscopy reveal oleic-acid-induced structural changes in intercellular lipid layers of the skin. *Optics letters* 29:2013-2015.
17. Liu Y, Chen HC, Yang SM, Sun TL, Lo W, Chiou LL, et al. (2007) Visualization of hepatobiliary excretory function by intravital multiphoton microscopy. *Journal of biomedical optics* 12:014014.
18. Sheu HM, Tsai JC, Lin TK, Wong TW, Lee JY (2003) Modified Nile red staining method for improved visualization of neutral lipid depositions in stratum corneum. *Journal of the Formosan Medical Association* 102:656-660.
19. Madison KC, Swartzendruber DC, Wertz PW, Downing DT (1987) Presence of intact intercellular lipid lamellae in the upper layers of the stratum corneum. *The Journal of investigative dermatology* 88:714-718.